Magnetic Circular Dichroism of Octaethylcorrphycene and Its Doubly Protonated and Deprotonated Forms

Alexander Gorski,[†] Emanuel Vogel,[‡] Jonathan L. Sessler,[§] and Jacek Waluk*[,†]

Institute of Physical Chemistry, Polish Academy of Sciences, Kasprzaka 44, 01-224 Warsaw, Poland, Institut für Organische Chemie der Universität, Greinstrasse 4, D-50939 Köln, Germany, and Department of Chemistry, Institute of Cellular and Molecular Biology, The University of Austin, Austin, Texas 77204-5641

Received: January 17, 2002; In Final Form: May 9, 2002

Electronic absorption and magnetic circular dichroism (MCD) spectra of 2,3,6,7,11,12,17,18-octaethylcorrphycene, a constitutional isomer of porphyrin, were recorded for the neutral, doubly protonated, and doubly deprotonated forms. The spectra closely resemble those of the parent porphyrin and are quite different from those of other porphyrin isomers such as porphycene and hemiporphycene. Theoretical considerations based on Michl's perimeter model allow one to understand the spectral properties observed within the series of porphyrin isomers composed of porphyrin, porphycene, hemiporphycene, and corrphycene. Differences in spectral features within members of the group are caused by varying orbital splitting patterns. In perimeter model terminology, corrphycene is a soft chromophore,with approximately equal energy splittings between the pairs of highest occupied and lowest unoccupied molecular orbitals (ΔHOMO $\approx$ ΔLUMO). As a consequence, a strong spectral sensitivity to structural peturbations is predicted for corrphycene. This behavior contrasts with what is expected for the porphyrin isomers porphycene and hemiporphycene, which are negative-hard chromophores (ΔHOMO < ΔLUMO). The experimentally observed excited-state characteristics are reproduced satisfactorily using time-dependent DFT (B3LYP/6-31G**) calculations. Finally, it is shown that the four-orbital model of Gouterman, which is widely used to interpret the spectral properties of porphyrin and its derivatives, is also applicable to corrphycene.

1. Introduction

Despite the long-known and all-important role played by porphyrins in many biological processes,[1] efforts devoted to studying constitutional isomers of porphyrin are less than two decades old. This area of research started with the synthesis of porphycene,[2] one of the eight (including porphyrin) possible "nitrogen-in" structures consisting of four pyrrole units linked in different ways by $-(CH)_n-$ bridges. Formally, these isomers are called porphyrins-(k.l.m.n.), where the indices denote the number of sp^2-hybridized bridging carbon atoms (methines) between the [(k + l + m + n) = 4] adjacent pyrrole units. In this notation, the parent compound is named porphyrin-(1.1.1.1), whereas porphycene is porphyrin-(2.0.2.0). In recent years, successful syntheses of alkyl derivatives of three more isomers have been reported. The (2.1.0.1) isomer was named corrphycene,[3] the (2.1.1.0) structure was called hemiporphycene,[4] and the term isoporphycene was coined for porphyrin-(3.0.1.0).[5] The structures are shown in Chart 1.

Porphyrin isomers, which have been important in fundamental resesarch, are now being studied with regard to their potential use in various areas ranging from the design of artificial photosynthetic systems,[6] sensors,[7] molecular optoelectronic devices,[8] photoswitches,[9] optical memories[10] and conductive polymers[11] to applications in photodynamic therapy.[12] In fact, porphycene has already been shown to be a very promising phototherapeutic agent candidate.[13] Because all of these techniques rely on the combined use of a chemical substance and light, a prerequisite for a successful application is a detailed understanding of the spectroscopy and photophysics of the lowest excited electronic states.

CHART 1: (Left to Right) (Top) Porphyrin, Porphycene; (Bottom) Hemiporphycene, Corrphycene, and Isoporphycene

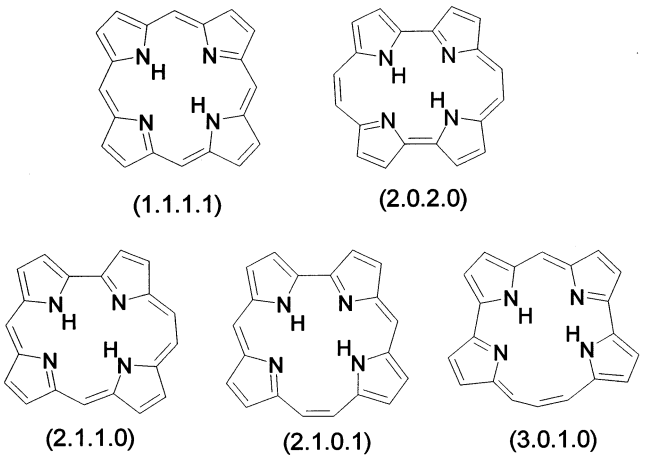

Several years ago, we carried out a theoretical analysis of the electronic structure of porphyrin isomers[14] that involved the use of a simple perimeter model.[15,16] In particular, predictions were made regarding the electronic absorption and magnetic circular dichroism (MCD) spectra. Of the various synthetic isomers now in existence, only porphycene existed then. However, recent synthetic advances and the availability of

* Corresponding author. E-mail: waluk@ichf.edu.pl. Tel: +4822 632 7269. Fax: +48 391 20 238.
[†] Polish Academy of Science.
[‡] Institut für Organische Chemie der Universität.
[§] The University of Austin.

10.1021/jp0201579 CCC: $22.00
Published on Web 08/09/2002

CHART 2: trans Tautomeric Form of 1

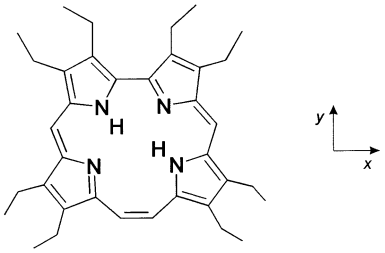

1

several porphyrin isomers in appreciable quantities now make it possible to check our theoretical predictions for a more diverse set of compounds. In this paper, we report and analyze the electronic absorption and MCD spectra of neutral, doubly deprotonated, and doubly protonated 2,3,6,7,11,12,17,18-octaethylcorrphycene (**1**, Chart 2). Our original theoretical analysis led to the conclusion that corrphycene should closely resemble the parent porphyrin with regard to the arrangement of the frontier molecular orbitals and, as a consequence, the pattern of its absorption and MCD spectra. The present experimental findings are in full agreement with this prediction. Specifically, they confirm, in the terminology of Michl's perimeter model, the soft chromophore character of corrphycene, a finding that is the result of a nearly equal energy separation between the two highest occupied and two lowest unoccupied π molecular orbitals (ΔHOMO $\approx$ ΔLUMO). In a separate paper,[17] we demonstrate that another recently synthesized porphyrin isomer, hemiporphycene, has a completely different character, being a negative-hard chromophore (ΔHOMO < ΔLUMO) by analogy to the previously investigated porphycene molecule.[18]

Michl's perimeter model is closely related to Gouterman's four-orbital model,[19] an approach successfully used for the analysis of the excited states of porphyrins. In this paper, we check the applicability of the four-orbital model to corrphycene and show that it works as well as it does for the parent system, porphyrin.

2. Experimental and Computational Details

The synthesis and purification of **1** have been described elsewhere.[4] Spectral-grade solvents (Merck) were used and were checked for the presence of fluorescing impurities. The spectra of the neutral and doubly protonated forms were measured in acetonitrile; the dication was produced by adding an excess of perchloric acid to acetonitrile solutions. The dianionic form was obtained in KOH-saturated dimethyl sulfoxide (DMSO). Absorption spectra were recorded on a Shimadzu UV3100 spectrophotometer. Magnetic circular dichroism (MCD) spectra were measured on a JASCO J-715 spectropolarimeter. Two different home-built magnets, a permanent magnet (field strength 2.9 kG) and an electromagnet (field intensity variable in the range 0−5 kG), were used. The difference between the spectra recorded with the opposite directions of the magnetic field was used to enhance the MCD signal and to minimize the baseline artifacts. The values of the Faraday *B* terms were extracted by integration from the isotropic solution spectra using the method of moments

$$B = -33.53^{-1} \int \mathrm{d}\tilde{\nu}\, [\Theta]_M/\tilde{\nu}$$

where $[\Theta]_M$ is the magnetically induced molar ellipticity per unit magnetic field (in units of deg L m^{-1} mol^{-1} G^{-1}) and $\tilde{\nu}$ is the wavenumber.

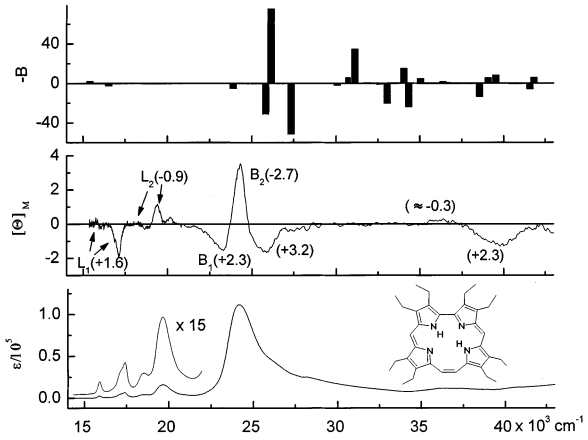

Figure 1. (Bottom) electronic absorption; (middle) MCD spectra with the values of *B* terms ($D^2 \times m_B/cm^{-1}$) given in parentheses; and (top) results of INDO/S calculations for **1**. The height of the bars reflects the calculated values of *B* terms. The spectra were recorded in acetonitrile solution at 293 K.

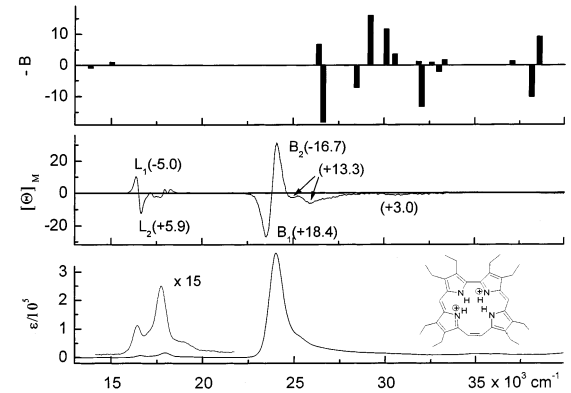

Figure 2. (Bottom) electronic absorption; (middle) MCD spectra; and (top) results of INDO/S calculations for the doubly protonated form of **1**. The spectra were recorded in a solution of acetonitrile containing a small amount of perchloric acid at 293 K. See the caption of Figure 1 for details.

The properties of the excited electronic singlet states were calculated for parent corrphycene and its charged forms using time-dependent density functional theory (TD-B3LYP/6-31G**) implemented in the Gaussian 98 program package.[20] Prior to excited-state calculations, the geometry of each structure was optimized using the same model. The Hessian matrix was checked for the absence of negative frequencies to ensure that the calculated structure corresponds to a real minimum. For the neutral and ionic forms of the octaethyl derivative, we performed INDO/S calculations,[21] which allowed us to calculate the values of the Faraday *B* terms. The structures were initially optimized using the AM1[22] or PM3[23] method.

3. Results and Discussion

Absorption and MCD spectra, as well as the results of the INDO/S calculations, are shown in Figures 1−3 for the neutral molecule, the doubly protonated form, and the dianion, respectively. The absorption and MCD patterns are similar in all three cases. Two weak transitions are observed in the visible region (Q bands), followed by strong transitions (Soret region). The MCD curves reveal the presence of an additional electronic transition lying close to the blue side of the higher Soret component. Additional weaker transitions are detected at higher energies.

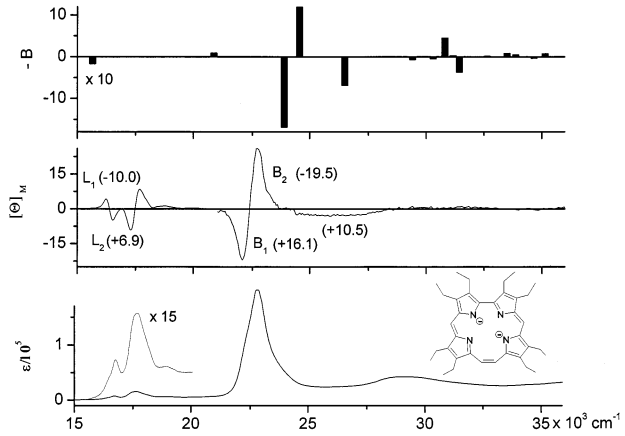

Figure 3. (Bottom) electronic absorption; (middle) MCD spectra; and (top) results of INDO/S calculations for the doubly deprotonated form of **1**. The spectra were recorded in KOH-saturated DMSO solution at 293 K. See the caption of Figure 1 for details.

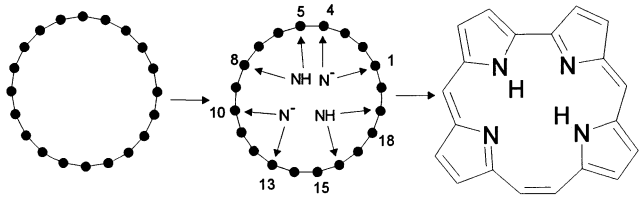

Figure 4. Formal derivation of corrphycene from an 18 π-electron perimeter, the [20]annulene dication.

In both the dication and dianion of **1**, the same pattern in the signs of *B* terms is observed, −, +, +,− (a negative *B* term corresponds to a positive MCD signal and vice versa). The same sequence is probably also obeyed in neutral **1**, although in this case, the 0−0 transitions of both L_1 and L_2 are extremely weak in the MCD spectra, which are clearly dominated by vibronic effects in this energy region. For all three forms, the MCD intensity is weaker for the Q bands than in the Soret region. This behavior is characteristic of porphyrin[24] and is completely opposite of that observed for porphycene[18] and hemiporphycene (the latter as an octaethyl derivative),[17] wherein the MCD signals of the first two excited states are much stronger than those of the Soret bands. The relative absorption intensities of the Q versus Soret bands are much stronger for porphycene and hemiporphycene, whereas corrphycene also resembles porphyrin in this respect. Finally, regular changes in the pattern of vibronic activity are observed along the series. In porphyrin and corrphycene, weak 0−0 bands for both Q transitions are followed by much stronger vibronic components. On the contrary, in porphycene, the 0−0 bands dominate. Hemiporphycene represents an intermediate case, with intensities of the 0−0 transitions being comparable to those of the strongest vibronic components.

To ground the above findings in theory, we have analyzed the properties of the lowest excited states in corrphycene using the so-called perimeter model,[15,16] an approach that has been used to explain the spectral behavior of other porphyrin isomers[17,18] and that of the parent system, porphyrin.[25] The starting point for these analyses is a $C_{20}H_{20}^{2+}$ $4N + 2 = 18$ π-electron perimeter. Formation of corrphycene is envisaged (Figure 4) as being due to structural perturbation caused by four kinds of bridges, two −NH and two $-N^-$ bridges in the neutral form, four −NH bridges in the dication, and four $-N^-$ bridges in the dianion. The perturbation arising from the bridges is expected to be the most pronounced in the latter instance because the lone pair orbitals of the $-N^-$ bridges are higher in energy than those of the NH group. Thus, the $-N^-$ bridges are stronger perturbers. In all cases, perturbation leads to splitting of the energies of the initially degenerate HOMO and LUMO pairs by an amount described by complex parameters *a* and *b*:

$$\Delta\mathrm{HOMO} = 2|a| \quad (1)$$

$$\Delta\mathrm{LUMO} = 2|b| \quad (2)$$

The components of the L and B electronic excited states, which are degenerate in the initial perimeter, become mixed. The resulting four electronic states are labeled L_1, L_2, B_1, and B_2 in order of increasing energy. The mixing can be described by two parameters, α and β:

$$\tan(2\alpha) = 2(|a| + |b|)/[E(\mathrm{B}) - E(\mathrm{L})] \quad (3)$$

$$\tan(2\beta) = 2(|a| - |b|)/[E(\mathrm{B}) - E(\mathrm{L})] \quad (4)$$

$E(\mathrm{B}) - E(\mathrm{L})$ is the energy difference between the L and B states in the parent perimeter. α and β can be approximated as

$$\alpha \approx (\Delta\mathrm{HOMO} + \Delta\mathrm{LUMO})/\{2[E(\mathrm{B}) - E(\mathrm{L})]\}$$

$$\beta \approx (\Delta\mathrm{HOMO} - \Delta\mathrm{LUMO})/\{2[E(\mathrm{B}) - E(\mathrm{L})]\}$$

Expressions were obtained for transition dipole strengths and polarizations and for the values of MCD terms.[15−16,18] The latter are given by

$$B(\mathrm{L}_1) = -B(\mathrm{L}_2) = -[m^2/(2\Delta L)](4\mu^- \sin^2\alpha \sin^2\beta + \mu^+ \sin 2\alpha \sin 2\beta) \quad (5)$$

$$B(\mathrm{B}_1) = -B(\mathrm{B}_2) = -[m^2/(2\Delta B)](4\mu^- \cos^2\alpha \cos^2\beta + \mu^+ \sin 2\alpha \sin 2\beta) \quad (6)$$

where it is assumed that ΔL, the separation between the two L states, and ΔB, the separation between the two B states, are much smaller than the L−B spacing.

It can be seen that the magnitudes of the *B* terms depend (through α and β) on the strength of the structural perturbation and on the electric (*m*) and magnetic (μ^- and μ^+) dipole contributions. The latter are functions of the size of the perimeter and of the number of π electrons ($4N + 2$). The contributions from both μ^- and μ^+ are usually negative, with the latter generally being an order of magnitude stronger.

The signs of MCD *B* terms for the four excited states are unequivocally predicted for the case in which $\Delta\mathrm{HOMO} > \Delta\mathrm{LUMO}$. The sequence is +, −, +, − for L_1, L_2, B_1, and B_2, respectively, no matter how strong the perturbation is. For $\Delta\mathrm{HOMO} < \Delta\mathrm{LUMO}$, the signs of the μ^- and μ^+ contributions to the *B* terms are opposite. For weak perturbations, the μ^+ contributions will dominate for the L_1 and L_2 states but not for the B_1 and B_2 transitions This leads to a −, +, +, − sequence. For sufficiently strong perturbations, contributions from μ^+ will also dominate the $B(\mathrm{B}_1)$ and $B(\mathrm{B}_2)$ terms, resulting in a −, +, −, + sequence of signs.

Chromophores that exhibit a negative $\Delta\mathrm{HOMO} - \Delta\mathrm{LUMO}$ difference have been named "negative-hard". The first part of this term indicates the sign of $B(\mathrm{L}_1)$, and the second, a general insensitivity to structural perturbations. By analogy, the condition $\Delta\mathrm{HOMO} > \Delta\mathrm{LUMO}$ corresponds to the case of a positive-hard chromophore.

For analytical and structural applications, the most interesting case involves soft chromophores, which are characterized by $\Delta\mathrm{HOMO} \approx \Delta\mathrm{LUMO}$. In such systems, $\beta \approx 0$, and the MCD signal in the region of L transitions should be very weak. It

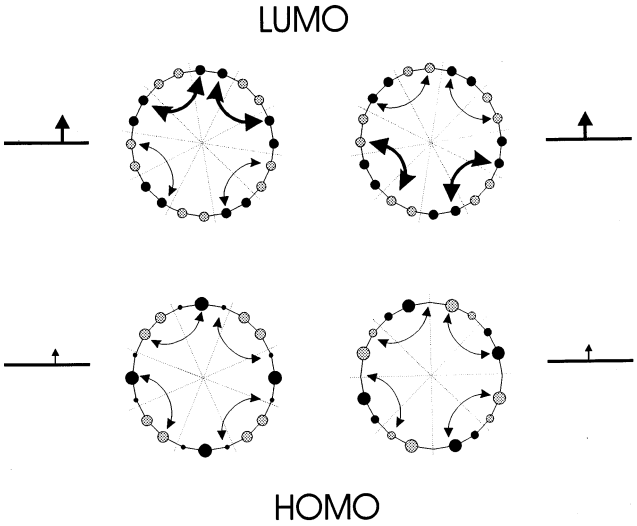

Figure 5. Shapes and nodal planes of the HOMO and LUMO orbitals of the parent $C_{20}H_{20}^{2+}$ perimeter and the predicted response to the perturbation corresponding to the formation of corrphycene.

may also be dominated in this range by effects such as vibronic coupling that are not taken into account in the perimeter model. Inspection of the MCD spectra of **1** (Figures 1−3) shows that these latter effects cannot be ignored; for the neutral and doubly protonated forms, the MCD intensity of the vibronic components is much stronger than that of the 0−0 bands. A similar situation has been encountered in porphyrins.[24]

Contrary to what is expected for the L bands, the intensity of the MCD B transitions should be quite strong in a soft chromophore, and the signs, which are dominated by μ^- contributions, are easy to predict. The *B* term should be positive for B_1 and negative for B_2. This is indeed observed in all three forms of **1**.

Another consequence of the soft character of the corrphycene chromophore is a weak absorption intensity in the Q region. The intensity ratio of the Q versus Soret bands is very small. This is analogous to what is seen for porphyrin[24] but is contrary to what is observed for the hard chromophores hemiporphycene[17] and porphycene.[18]

The soft chromophore character of corrphycene can be derived easily by considering the shape of the molecular orbitals of the parent perimeter and then predicting the response of each orbital to the structural perturbations that formally lead to corrphycene. This process is shown in Figure 5. The bridging will have a significant effect on the energy of a molecular orbital if (i) the LCAO coefficients at the bridging positions are large and (ii) the bridging group does not lie in the nodal plane. None of the HOMO orbitals should undergo a significant shift upon bridging, and thus no significant splitting is expected. The two LUMO orbitals are pushed to higher energies, each by the same amount. Again, no splitting is expected. The same situation is encountered for porphyrin. However, the topology of porphycene dictates completely different behavior; four bridges raise the energy of one of the LUMO orbitals, leaving the other orbital unaffected.[14] In hemiporphycene, three bridges affect the energy of one component of the LUMO pair, whereas only one bridge raises the energy of the other component.[14,17] These simple considerations explain why porphyrin and corrphycene are soft chromophores, whereas porphycene and hemiporphycene are negative-hard in character, with the former being more so than the latter.

The above qualitative analysis is supported quantitatively by calculations. We previously predicted the approximate equality of ΔHOMO and ΔLUMO in corrphycene using the PPP method.[14] More sophisticated treatments, such as those employed in this work, lead to the same conclusion regardless of whether AM1, PM3, INDO/S, or Kohn−Sham orbitals are used. Specifically, by using B3LYP/6-31G** calculations for the nonalkylated species, we obtained 0.03 and 0.07 eV for the values of ΔHOMO and ΔLUMO, respectively, in the neutral form of corrphycene. The corresponding values for the dianion are 0.07 and 0.05 eV. For the dication, two different ground-state structures, with energies separated by 3.99 kcal/mol, were obtained (Figure 6). Neither form is calculated as being flat, but they differ in their degrees of nonplanarity and in the way in which the inner protons are tilted out of the molecular plane. The calculations gave 0.06 and 0.07 eV for the HOMO and LUMO splittings, respectively in the lower-energy form (a) and 0.01 and 0.04 eV for the splittings in the other structure (b). The near equality of ΔHOMO and ΔLUMO was also predicted by PM3 calculations performed for the molecule under study, namely, octaethylcorrphycene. However, for hemiporphycene and porphycene, all of the computational methods that were used yielded ΔHOMO < ΔLUMO.

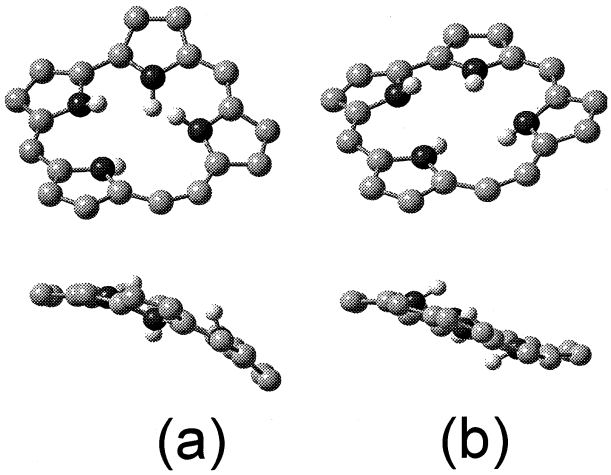

Figure 6. Structures of two doubly protonated forms of corrphycene calculated by B3LYP/6−31**. The lower energy was obtained for form (a).

For nearly equal ΔHOMO and ΔLUMO values, correct reproduction of the MCD signs is not an easy task, as illustrated in Figures 1−3, which show the results of INDO/S calculations. For the neutral corrphycene, the results are correct for all four perimeter excited states and also for an additional nearby higher-energy transition. However, the signs are not correctly predicted for the L transitions in the dianion. For the dication, the situation is even worse, which may be due to the presence of two nonplanar structures and possible solute−solvent interactions leading to changes in the geometry and location of excited states. Actually, we note that the MCD intensity is stronger for the dication than for the neutral molecule and is similar to that for the anion. This result is somewhat unexpected, given that the −NH groups are weaker perturbers than the $-N^-$ bridges. However, the nonplanarity of this system may enhance the effect of perturbation and make the dication a "harder" chromophore. In any event, the MCD results combined with the ΔHOMO and ΔLUMO values obtained for the two forms of the dication favor structure (b) in Figure 6.

We have also calculated the excited-state energies for the neutral and ionic forms of the parent (i.e., substitutent-free) corrphycene using time-dependent density functional theory (TD-DFT). The results are summarized in Tables 1−4. Differ-

TABLE 1: Calculated (TD-B3LYP/6-31G) Electronic States of Neutral Corrphycene and the Energies Observed for the Octaethyl Derivative**

	calcd energy[a] (10^3 cm^{-1})	oscillator strength	α[b] (deg)	dominant configuration[c]	exptl energy[d] (10^3 cm^{-1})
1	18.9	0.0013	−44	0.52 (1−1) + 0.48 (2−2)	15.9 (L_1)
2	19.8	0.0005	+79	0.49 (2−1) − 0.48 (1−2)	18.5 (L_2)
3	25.6	0.293	−17	0.36 (4−1) + 0.31 (2−2)	23.3 (B_1)
4	27.5	0.533	+69	0.31 (1−2)	24.3 (B_2)
5	27.7	0.040	+67	0.56 (3−2)	
6	28.4	0.243	+18	0.54 (3−1)	25.9
7	29.3	0.265	−21	0.51 (4−2)	
8	30.3	0.559	−80	0.41 (4−2)	
9	31.9	0.000	*nπ**[e]	0.57 (7−2)	
10	32.4	0.000	*nπ**	0.63 (8−1)	
11	33.4	0.078	+8	0.66 (5−1)	
12	33.7	0.000	*nπ**	0.56 (7−1)	
13	34.2	0.073	−33	0.47 (6−2)	
14	34.6	0.021	−85	0.56 (5−2)	
15	34.7	0.000	*nπ**	0.63 (8−2)	
16	34.9	0.060	−80	0.47 (6−2)	∼36.0
17	36.9	0.034	−7	0.56 (1−3)	
18	37.2	0.049	−3	0.50 (2−3)	
19	37.9	0.051	+1	0.50 (10−1)	
20	39.6	0.201	−3	0.47 (10−2)	39.9

[a] Calculated for the unsubstituted parent molecule. [b] Angle between the transition moment and the horizontal molecular axis *x*; positive values correspond to the anticlockwise rotation from *x* (see Chart 2). [c] Occupied orbitals are numbered 1, 2, ... downward, and unoccupied orbitals, −1, −2, ... upwards. [d] Experimental results for a room-temperature solution of **1**. [e] *nπ** transition, out-of-plane polarization.

TABLE 2: Calculated (TD-B3LYP/6-31G) Electronic States of the Corrphycene Dianion and Observed Values for the Octaethyl Derivative[a]**

	calcd energy (10^3 cm^{-1})	oscillator strength	dominant configuration	exptl energy[b] (10^3 cm^{-1})
1	18.5	0.0033	0.52 (1−1)	16.2 (L_1)
2	18.8	0.0001	0.50 (1−2) + 0.46 (2−1)	16.6 (L_2)
3	20.2	0.003	0.63 (3−1)	
4	20.4	0.012	0.61 (3−2)	
5	23.4	0.031	0.38 (1−2) + 0.38 (2−1)	22.1 (B_1)
6	24.6	0.243	0.42 (4−2) − 0.30 (2−2)	22.7 (B_2)
7	25.2	0.011	0.67 (4−1)	∼26
8	25.9	0.109	0.53 (4−2)	
9	28.1	0.156	0.50 (7−1)	
10	28.2	0.117	0.41 (7−1)	
11	28.3	0.003	0.64 (7−2)	
12	28.4	0.007	0.63 (5−2)	
13	29.4	0.424	0.54 (6−2)	∼29
14	29.5	0.000	0.63 (6−1)	
15	31.6	0.051	0.63 (8−2)	
16	31.7	0.121	0.63 (8−1)	
17	32.9	0.024	0.55 (10−1)	
18	33.2	0.043	0.55 (9−1)	
19	33.3	0.005	0.59 (10−2)	
20	33.7	0.097	0.44 (1−3)	

[a] See caption of Table 1 for details. [b] Room-temperature solution of **1** in DMSO saturated with KOH.

ences between the experimentally derived and calculated energy values are similar to those reported previously for porphyrin and derivatives.[26,27] The calculated transition energies are about 2000−3000 cm^{-1} too high. This may be due, in part, to the neglect of alkyl substituents. It has been recently demonstrated[26] that the excitation energies calculated for 1,3,5,7-tetramethyl-2,4,6,8-tetraethyl-substituted magnesium porphyrin are about 0.2−0.3 eV smaller than those computed for the nonalkylated molecule. The splittings between L and B transitions are reproduced with much better accuracy. Overall, TD-DFT calculations reveal a significant improvement over INDO/S analyses, in particular, when predicting the energy differences between the Q transitions in the charged forms.

TABLE 3: Calculated (TD-B3LYP/6-31G) Electronic States in Form a of the Doubly Protonated Corrphycene[a] and Experimental Values Obtained for the Octaethyl Derivative[b]**

	calcd energy (10^3 cm^{-1})	oscillator strength	dominant configuration	exptl energy[c] (10^3 cm^{-1})
1	18.5	0.0033	0.52 (1−1) − 0.49 (2−2)	16.4 (L_1)
2	18.5	0.0000	0.51 (1−2) + 0.51 (2−1)	16.7 (L_2)
3	28.2	1.020	0.40 (2−2)	23.5 (B_1)
4	28.4	1.059	0.37 (1−2) − 0.37 (2−1)	24.1 (B_2)
5	30.2	0.005	0.68 (3−1)	25.9
6	30.6	0.045	0.59 (6−1)	
7	30.9	0.081	0.62 (5−2)	∼31
8	31.0	0.034	0.63 (4−2)	
9	31.6	0.038	0.56 (4−1)	
10	31.7	0.072	0.67 (5−1)	
11	31.8	0.018	0.63 (3−2)	
12	32.5	0.071	0.64 (6−2)	
13	36.0	0.000	0.53 (7−2)	
14	36.7	0.005	0.59 (7−1)	
15	36.8	0.000	0.60 (2−3)	
16	37.7	0.101	0.51 (8−2)	
17	38.5	0.000	0.54 (1−4)	
18	39.3	0.036	0.49 (2−4)	
19	44.3	0.033	0.44 (2−4)	
20	44.7	0.016	0.34 (1−4)	

[a] See Figure 6. [b] See caption of Table 1 for details. [c] Room-temperature solution of **1** in acetonitrile containing perchloric acid.

TABLE 4: Calculated (TD-B3LYP/6-31G) Electronic States of Form b of the Doubly Protonated Corrphycene[a] and Experimental Values Obtained for the Octaethyl Derivative[b]**

	calcd energy (10^3 cm^{-1})	oscillator strength	dominant configuration	exptl energy[c] (10^3 cm^{-1})
1	18.5	0.0002	0.42 (1−1) + 0.41 (2−2)	16.4 (L_1)
2	18.8	0.0004	0.41 (2−1) − 0.41 (1−2)	16.7 (L_2)
3	28.4	1.041	0.37 (2−2) − 0.35 (1−1)	23.5 (B_1)
4	28.6	0.976	0.34 (1−2) + 0.34 (2−1)	24.1 (B_2)
5	29.5	0.184	0.57 (3−1)	25.9
6	29.7	0.066	0.58 (4−2)	
7	30.7	0.087	0.46 (3−2)	∼31
8	30.8	0.025	0.53 (4−1)	
9	31.8	0.011	0.64 (6−1)	
10	31.8	0.022	0.64 (5−2)	
11	32.6	0.047	0.62 (5−1)	
12	33.3	0.054	0.65 (6−2)	
13	36.1	0.000	0.43 (7−2)	
14	36.8	0.001	0.59 (1−3)	
15	37.2	0.000	0.51 (7−1)	
16	37.7	0.071	0.46 (2−3)	
17	38.4	0.006	0.52 (2−4)	
18	38.9	0.053	0.54 (1−4)	
19	44.2	0.003	0.38 (1−4)	
20	44.6	0.012	0.61 (2−4)	

[a] See Figure 6. [b] See caption of Table 1 for details. [c] Room-temperature solution of **1** in acetonitrile containing perchloric acid.

In general, the assignment of the electronic transitions solely on the basis of the MCD spectra is not possible because the reversal of the ordering in the pairs of L and B levels would not lead to a change in the pattern of the MCD signs. However, the combined use of the absorption, MCD, and calculation results allows us to propose tentative assignments for the four lowest observed electronic transitions. These are given in Tables 1−4. Interestingly, both TD-DFT and INDO/S predict that the lowest-energy transition in **1** is polarized approximately along the NH···NH direction, whereas the second lowest transition is polarized at a large angle with respect to the NH···NH direction. This is analogous to the situation encountered in porphyrin and porphycene. A detailed study of transition moment directions

TABLE 5: Values of the Sums of Squares of the Four CI Coefficients Describing the Contributions from Single Excitations Considered in the Four-Orbital Model[a]

	neutral form		dication		dianion	
L_1	15.4 (0.005)	0.95	13.9 (0.041)	0.96	15.7 (0.009)	0.97
L_2	16.5 (0.009)	0.98	15.0 (0.001)	0.95	20.9 (0.050)	0.97
B_1	26.2 (1.92)	0.75	26.4 (2.52)	0.92	23.9 (2.13)	0.87
B_2	27.4 (1.45)	0.51	26.7 (2.82)	0.85	24.5 (0.40)	0.83

[a] INDO/S calculations involved a 14 × 14 CI basis set.

in which the techniques of polarized spectroscopy are used is under way.

The analysis of absorption and MCD results presented in this work is predicated on the use of a simple perimeter model. This model, in turn, is closely related to Gouterman's four-orbital scheme.[19] We decided to check the accuracy of the latter approach when applied to corrphycene by performing large CI semiempirical calculations and subsequently inspecting the contributions from the four excitations involving the HOMO and LUMO orbitals. Table 5 presents the values of the sums of squares of the four CI coefficients that describe the excitations involving the two HOMOs and two LUMOs. The values of these parameters provide a check on the accuracy of an approach that relies on only four orbitals. The better the model, the closer the values should be to unity. It can be seen that the four-orbital approach works perfectly for the L states and quite satisfactorily for all of the Soret transitions except for one case involving the B_2 component in the neutral form. Similar results have been obtained for porphyrin,[28] porphycene,[28] dibenzoporphycenes,[28] and smaragdyrins.[29] However, in rosarin, a hexapyrrolic macrocyle, the four-orbital model is completely inadequate; here, symmetry dictates that a 3 × 3 HOMO and LUMO basis set be applied for a proper description of the lowest excited states.[30]

4. Summary and Conclusions

Both experiment and theory unequivocally demonstrate the soft character of corrphycene as a chromophore. As a consequence, corrphycene displays spectral features that are very similar to those of porphyrin and very different from those of the negative-hard chromophores porphycene and hemiporphycene. Nonetheless, it is important to appreciate that the approximate equality of orbital splittings observed for corrphycene can be easily destroyed by structural perturbations such as substitution. The sign of the resulting $\Delta\text{HOMO} - \Delta\text{LUMO}$ difference is predicted to be strongly position-dependent. This could make MCD spectroscopy an attractive tool for the study and characterization of functionalized corrphycene derivatives.

With the completion of the present study, most of the constitutional isomers of porphyrin synthesized to date have been studied by MCD. Only isoporphycene[5] and "N-confused" or "inverted" porphyrins[31] remain to be analyzed in this way. Here, use of the perimeter model leads to the prediction that both molecules should be considered to be soft or nearly soft chromophores. To the extent that this is proven to be true, MCD spectroscopy could to be a valuable tool in analyzing preferred conformations or tautomeric structures. We are currently using MCD to study tautomeric equilibria in an inverted porphyrin.

Acknowledgment. We thank Professor J. Frelek from the Institute of Organic Chemistry of the Polish Academy of Sciences for allowing us to use the spectropolarimeter. We acknowledge Professor J. Michl and Dr. J. Downing (University of Colorado, Boulder) for allowing us to use their version of the INDO/S program. This work was partially sponsored by KBN grants 3T09A 06314 and 7T09A 2420. Support to J.L.S. under the terms of NSF grant CHE 9725399 is also gratefully acknowledged. Some of the results of this work were obtained using the computer resources of the Interdisciplinary Centre for Mathematical and Computational Modelling (ICM) of the Warsaw University.

References and Notes

(1) Battersby, A. R.; Fookes, C. J. R.; Matcham, G. W. J.; McDonals, E. *Nature (London)* **1980**, *285*, 17.

(2) Vogel, E.; Köcher, M.; Schmickler, H.; Lex, J. *Angew. Chem., Int. Ed. Engl.* **1986**, *25*, 257.

(3) Sessler, J. L.; Brucker, E. A.; Weghorn, S. J.; Kisters, M.; Schäfer, M.; Lex, J.; Vogel, E. *Angew. Chem., Int. Ed. Engl.* **1994**, *33*, 2308.

(4) (a) Callot, H. J.; Rohrer, A.; Tschamber, T.; Metz, B. *New J. Chem.* **1995**, *19*, 155. (b) Vogel, E.; Bröring, M.; Weghorn, S. J.; Scholz, P.; Deponte, R.; Lex, J.; Schmickler, H.; Schaffner, K.; Braslavsky, S. E.; Müller, M.; Pörting, S.; Fowler, C. J.; Sessler, J. L. *Angew. Chem., Int. Ed. Engl.* **1997**, *36*, 1651.

(5) (a) Vogel, E.; Bröring, M.; Erben, C.; Demuth, R.; Lex, J.; Nendel, M.; Houk, K. N. *Angew. Chem., Int. Ed. Engl.* **1997**, *36*, 353. (b) Vogel, E.; Scholz, P.; Demuth, R.; Erben, C.; Bröring, M.; Schmickler, H.; Lex, J.; Hohlneicher, G.; Bremm, D.; Wu, Y.-D. *Angew. Chem., Int. Ed.* **1999**, *38*, 2919.

(6) (a) Gust, D.; Moore, T. A.; Moore, A. L.; Lee, S.-J.; Bittersmann, E.; Luttrull, D. K.; Rehms, A. A.; DeGraziano, J. M.; Ma, X. C.; Gao, F.; Belford, R. E.; Trier, T. T. *Science (Washington, D.C.)* **1990**, *248*, 199. (b) Imahori, H.; Arimura, M.; Hanada, T.; Nishimura, Y.; Yamazaki, I.; Sakata, Y.; Fukuzumi, S. *J. Am. Chem. Soc.* **2001**, *123*, 335.

(7) Deviprasad, G. R.; D'Souza, F. *Chem. Commun.* **2000**, 1915.

(8) Wagner, R. W.; Lindsey, J. S.; Seth, J.; Palaniappan, V.; Bocian, D. F. *J. Am. Chem. Soc.* **1996**, *118*, 3966.

(9) Reddy, D. R.; Maiya, B. G. *Chem. Commun.* **2001**, 117.

(10) Drobizhev, M.; Sigel, C.; Rebane, A. *J. Lumin.* **2000**, *86*, 391.

(11) Collman, J. P.; McDevitt, J. T.; Yee, G. T.; Leidner, C. R.; McCullough, L. G.; Little, W. A.; Torrance, J. B. *Proc. Natl. Acad. Sci. U.S.A.* **1986**, *83*, 4581.

(12) Bonnet, R. *Chem. Soc. Rev.* **1995**, 19.

(13) (a) Abels, C.; Szeimies, R.-M.; Steinbach, P.; Richert, C.; Goetz, A. E.; *J. Photochem. Photobiol., B* **1997**, *40*, 305. (b) Fickweiler, S.; Abels, C.; Karrer, S.; Bäumler, W.; Landhalter, M.; Hofstädter, F.; Szeimies, R.-M. *J. Photochem. Photobiol., B* **1999**, *48*, 27. (c) Kessel, D.; Luo, Y. *J. Photochem. Photobiol., B* **1998**, *42*, 89. (d) Toledano, H.; Edrei, R.; Kimel, S. *J. Photochem. Photobiol., B* **1998**, *42*, 20. (e) Guardiano, M.; Biolo, R.; Jori, G.; Schaffner, K. *Cancer Lett.* **1989**, *44*, 1. (f) Gottfried, V.; Davidi, R.; Averbuj, C.; Kimel, S. *J. Photochem. Photobiol., B* **1995**, *30*, 115. (g) Segalla, A.; Fedelli, F.; Reddi, E.; Jori, G. *Int. J. Cancer* **1997**, *72*, 329.

(14) Waluk, J.; Michl, J. *J. Org. Chem.* **1991**, *56*, 2729.

(15) (a) Michl, J. *J. Am. Chem. Soc.* **1978**, *100*, 6801. (b) Michl, J. *J. Am. Chem. Soc.* **1978**, *100*, 6812. (c) Michl, J. *J. Am. Chem. Soc.* **1978**, *100*, 6819.

(16) Michl, J. *Tetrahedron* **1984**, *40*, 3845.

(17) Gorski, A.; Vogel, E.; Sessler, J. L.; Waluk, J. *Chem. Phys.*, in press.

(18) Waluk, J.; Müller, M.; Swiderek, P.; Köcher, M.; Vogel, E.; Hohlneicher, G.; Michl, J. *J. Am. Chem. Soc.* **1991**, *113*, 5511.

(19) Gouterman, M. *J. Mol. Spectrosc.* **1961**, *6*, 138. Gouterman, M.; Wagniere, G. H.; Snyder, L. C. *J. Mol. Spectrosc.* **1963**, 11, 108.

(20) Frisch, M. J.; Trucks, G. W.; Schlegel, H. B.; Scuseria, G. E.; Robb, M. A.; Cheeseman, J. R.; Zakrzewski, V. G.; Montgomery, J. A., Jr.; Stratmann, R. E.; Burant, J. C.; Dapprich, S.; Millam, J. M.; Daniels, A. D.; Kudin, K. N.; Strain, M. C.; Farkas, O.; Tomasi, J.; Barone, V.; Cossi, M.; Cammi, R.; Mennucci, B.; Pomelli, C.; Adamo, C.; Clifford, S.; Ochterski, J.; Petersson, G. A.; Ayala, P. Y.; Cui, Q.; Morokuma, K.; Malick, D. K.; Rabuck, A. D.; Raghavachari, K.; Foresman, J. B.; Cioslowski, J.; Ortiz, J. V.; Stefanov, B. B.; Liu, G.; Liashenko, A.; Piskorz, P.; Komaromi, I.; Gomperts, R.; Martin, R. L.; Fox, D. J.; Keith, T.; Al-Laham, M. A.; Peng, C. Y.; Nanayakkara, A.; Gonzalez, C.; Challacombe, M.; Gill, P. M. W.; Johnson, B. G.; Chen, W.; Wong, M. W.; Andres, J. L.; Head-Gordon, M.; Replogle, E. S.; Pople, J. A. *Gaussian 98*, revision A.6; Gaussian, Inc.: Pittsburgh, PA, 1998.

(21) Ridley, J. E.; Zerner, M. Z. *Theor. Chim. Acta* **1973**, *32*, 111.

(22) Dewar, M. J. S.; Zoeblisch, E. G.; Healy, E. F.; Stewart, J. J. P. *J. Am. Chem. Soc.* **1985**, *107*, 3902.

(23) Stewart, J. J. P. *J. Comput. Chem.* **1989**, *10*, 209, 221.

(24) (a) Keegan, J. D.; Stolzenberg, A. M.; Lu, Y.-Ch.; Linder, R. E.; Barth, G.; Bunnenberg, E.; Djerassi, C.; Moscowitz, A. *J. Am. Chem. Soc.* **1981**, *103*, 3201. (b) Keegan, J. D.; Stolzenberg, A. M.; Lu, Y. Ch.; Linder, R. E.; Barth, G.; Moscowitz, A.; Bunnenberg, E.; Djerassi, C. *J. Am. Chem.*

Soc. **1982**, *104*, 4305. (c) Keegan, J. D.; Stolzenberg, A. M.; Lu, Y. Ch.; Linder, R. E.; Barth, G.; Moscowitz, A.; Bunnenberg, E.; Djerassi, C. *J. Am. Chem. Soc.* **1982**, *104*, 4317. (d) Goldbeck, R. A.; Tolf, B. R.; Wee, A. G. H.; Shu, A. Y. L.; Records, R.; Bunnenberg, E.; Djerassi, C. *J. Am. Chem. Soc.* **1986**, *108*, 6449.

(25) Goldbeck, R. A. *Acc. Chem. Res.* **1988**, *21*, 95.

(26) Sundholm, D. *Chem. Phys. Lett.* **2000**, *317*, 392.

(27) (a) Rubio, M.; Roos, B. O.; Serrano-Andrés, L.; Merchán, M. *J. Chem. Phys.* **1999**, *110*, 7202. (b) Serrano-Andrés, L.; Merchán, M.; Rubio, M.; Roos, B. O. *Chem. Phys. Lett.* **1998**, *295*, 195. (c) Gwaltney, S. R.; Bartlett, R. J. *J. Chem. Phys.* **1998**, *108*, 6790. (d) Tretiak, S.; Chernyak, V.; Mukamel, S. *Chem. Phys. Lett.* **1998**, *297*, 357. (e) Hasegawa, J.; Ozeki, Y.; Ohkawa, K.; Hada, M.; Nakatsuji, H. *J. Phys. Chem. B* **1998**, *102*, 1320. (f) Hasegawa, J.; Hada, M.; Nonoguchi, M.; Nakatsuji, H. *Chem. Phys. Lett.* **1996**, *250*, 159.

(28) Dobkowski, J.; Galievsky, V.; Starukhin, A.; Vogel, E.; Waluk, J. *J. Phys. Chem. A* **1998**, *102*, 4996.

(29) Gorski, A.; Lament, B.; Davis, J. M.; Sessler, J.; Waluk, J. *J. Phys. Chem. A* **2001**, *105*, 4992.

(30) Lament, B.; Dobkowski, J.; Sessler, J. L.; Weghorn, S. J. Waluk, J. *Chem.—Eur. J.* **1999**, *10*, 3039.

(31) Latos-Grażyński, L. In *The Porphyrin Handbook*; Kadish, K. M., Smith, K. M., Guillard, R., Eds.; Academic Press: San Diego, CA, 2000; Vol. 2, Chapter 14.